2-12-2019

Cd(II)- and Pb(II)-Induced Self-Assembly of Peripheral Membrane Domains from Protein Kinase C

Taylor R. Cole

Samuel G. Erickson

Krystal A. Morales

MinWoo Sung

Andreas Holzenburg

See next page for additional authors

Authors

Taylor R. Cole, Samuel G. Erickson, Krystal A. Morales, MinWoo Sung, Andreas Holzenburg, and Tatyana I. Igumenova

HHS Public Access

Author manuscript

Biochemistry. Author manuscript; available in PMC 2021 March 22.

Published in final edited form as:

Biochemistry. 2019 February 12; 58(6): 509–513. doi:10.1021/acs.biochem.8b01235.

Cd(II)- and Pb(II)-Induced Self-Assembly of Peripheral Membrane Domains from Protein Kinase C

Taylor R. Cole[†], **Samuel G. Erickson**[†], **Krystal A. Morales**[†], **MinWoo Sung**[‡], **Andreas Holzenburg**[§], **Tatyana I. Igumenova**[*,†]

[†]Department of Biochemistry and Biophysics, Texas A&M University, 300 Olsen Boulevard, College Station, Texas 77843, United States

[‡]Department of Biology, Texas A&M University, College Station, Texas 77843, United States

[§]School of Medicine, University of Texas Rio Grande Valley, Harlingen, Texas 78550, United States

Abstract

Cd^{2+} and Pb^{2+} are xenobiotic heavy metal ions that use ionic mimicry to interfere with the cellular function of biomacromolecules. Using a combination of SAXS, electron microscopy, FRET, and solution NMR spectroscopy, we demonstrate that treatment with Cd^{2+} and Pb^{2+} causes self-assembly of protein kinase C regulatory domains that peripherally associate with membranes. The self-assembly process successfully competes with ionic mimicry and is mediated by conserved protein regions that are distinct from the canonical Ca^{2+}-binding motifs of protein kinase C. The ability of protein oligomers to interact with anionic membranes is enhanced compared to the monomeric species. Our findings suggest that metal-ion-dependent peripheral membrane domains can be utilized for generating protein–metal-ion nanoclusters and serve as biotemplates for the design of sequestration agents.

Cadmium (Cd) and lead (Pb) are potent environmental toxins whose harmful effects on human health are well-documented.[1–4] Ionic mimicry is considered to be the primary mechanism through which these metal ions interfere with cellular processes. It can involve (i) the cellular uptake of Cd^{2+} and Pb^{2+}, through hijacking the transporters responsible for the import of essential metal ions[5–7] and (ii) intracellular competition for metal-ion-binding sites of proteins involved in cellular signaling,[8–13] metabolism,[14,15] and metal-ion homeostasis.[16,17] Here, we report another mode of Cd^{2+} and Pb^{2+} action that coexists and successfully competes with ionic mimicry. The phenomenon in question is the M^{2+} (M = Cd, Pb)-mediated self-assembly of peripheral membrane regions that belong to the lipid- and

[*]**Corresponding Author:** tigumenova@tamu.edu.

Supporting Information

The Supporting Information is available free of charge on the ACS Publications website at DOI: 10.1021/acs.biochem.8b01235. Experimental procedures, electron micrograph, fluorescence emission spectra, analytical gel filtration profiles, estimation of molecular mass from the size-exclusion chromatography, NMR spectra of C1B–C2 variants, sequence alignments, and histogram representation of sedimentation coefficients (PDF)

The authors declare no competing financial interest.

Ca^{2+}-activated α isoform of protein kinase C (PKC). Both Pb^{2+} and Cd^{2+} activate PKC.[8,18–20]

The N-term region (Figure 1A) controls the enzymatic activity of PKC: its membrane insertion in response to binding second messengers Ca^{2+} and diacylglycerol relieves the autoinhibition of the enzyme. The region comprises two types of peripheral membrane modules: the tandem conserved homology 1 (C1A and C1B) and conserved homology 2 (C2) domains. C1 domains are the treble-clef Zn^{2+} fingers. They bind membrane-embedded diacylglycerol as part of the PKC activation process (Figure 1B). The C2 domain in its metal-ion free state does not interact with membranes. Binding of Ca^{2+} to the negatively charged apical loop region drives the C2 domain to anionic membranes (Figure 1B). The divalent metal ions therefore play two distinct roles: Zn^{2+} ensures the structural integrity of the diacylglycerol-sensing C1 domains, while Ca^{2+} facilitates the C2 membrane insertion as part of the PKC activation process. We previously demonstrated that Pb^{2+} and Cd^{2+} bind to the loop regions of isolated C2 domains[9,10,21,22] with a high affinity and thereby can act as competitive inhibitors of Ca^{2+} binding.

To determine the effect of divalent metal ions on the N-term regulatory region of PKC, we conducted SAXS experiments (sections S1–3 and Table S2) on the 22.3 kDa C1B–C2 region from PKCα and the 30.6 kDa chimeric full regulatory region C1C2c that additionally contains the C1A domain from the γ isoform.[23] Three metal ions were used: Cd^{2+}, Pb^{2+}, and native activator Ca^{2+}. Unexpectedly, we found that Cd^{2+} and Pb^{2+} caused significant changes in protein morphology compared to Ca^{2+} (Figure 2A). Moreover, based on the similarity of the Cd^{2+} and Pb^{2+} scattering curves, we concluded that the effect of these metal ions on the N-term regulatory regions is similar.

Analysis of the pair-distance distribution functions, $P(r)$, revealed that interactions with Cd^{2+} and Pb^{2+} cause the self-assembly of the N-term regions. This is manifested in (i) a ~2-fold increase in the radius of gyration, R_g, and (ii) 2- to 3-fold increase in the maximum distance present in the scattering particle, D_{max}, both relative to the Ca^{2+}-bound species (Figure 2B). Estimation of the molecular mass produced the following values in kDa: 20 (Ca^{2+}/C1B–C2, monomer mass 22.3 kDa), 32 (Ca^{2+}/C1C2c, monomer mass 30.6 kDa), 310 (Cd^{2+}/ C1B–C2), 310 (Cd^{2+}/C1C2c), and 260 (Pb^{2+}/C1C2c). These data indicate that Ca^{2+}-complexed proteins remain mostly monomeric, whereas Cd^{2+} and Pb^{2+}-complexed proteins self-assemble with $n \sim 8–14$. The Pb^{2+}/C1B–C2 scattering curves were not suitable for quantitative analysis (section S3).

To evaluate the flexibility and shape of the protein complexes, we constructed dimensionless Kratky plots.[24] The plots of globular proteins converge to zero at high scattering angles and have a maximum of 1.1 at $qR_g = \sqrt{3}$. Ca^{2+}-complexed C1B–C2 and C1C2c lack these features and have a plateau-like region at high a qR_g that is typical of flexible multidomain proteins (Figure 2C). In contrast to Ca^{2+}, all Cd^{2+} and Pb^{2+} plots have maxima at ($\sqrt{3}$, 1.1) and show a significant decrease in intensity at high qR_g values. We conclude that the Ca^{2+}-complexed regulatory regions behave as flexible monomers in solution, consistent with their modular architecture and unstructured linkers. Interactions with Cd^{2+} and Pb^{2+} result in the formation of oligomeric species that are more globular in shape, with attenuated mobility of

the linker regions. For the rest of the work reported here, we used a 2-domain C1B–C2 membrane-binding region due to its favorable solubility properties.

We conducted negative-stain electron microscopy experiments to visualize the oligomers (Figure 3A,B; Ca^{2+} control, Figure S1). The overall globular (Cd^{2+}) and ellipsoidal (Pb^{2+}) shapes of C1B–C2 oligomers are evident from the inspection of characteristic class averages (bottom panel of Figure 3A,B). The Cd^{2+}-containing particles appear to be composed of 4 spherical densities, each with an estimated molecular mass of 80 kDa. Given that the molecular mass of the monomer is 22.3 kDa, this would correspond to a 320 kDa oligomer consisting of ~16 monomers. This is in good agreement with SAXS results. The footprint of Pb^{2+}-containing particles appears as two parallel ellipsoids, with each ellipsoid having an estimated molecular mass of ~40 kDa. This arrangement would produce an 80 kDa tetramer. The distributions of particle sizes are centered at ~12.5 and ~15.0 nm for the Pb^{2+}- and Cd^{2+}- containing particles, respectively (Figure 3C).

Protein-to-membrane FRET experiments (Figure 3D) demonstrated that both Pb^{2+} and Cd^{2+}-complexed C1B–C2 oligomers associate with anionic lipid membranes. This is manifested in the appearance of the dansyl emission peak upon addition of Pb^{2+} (Figure 3E) and Cd^{2+} (Figure 3F) to C1B–C2. Ca^{2+} control is given in Figure S2. EGTA treatment eliminated the dansyl peak, indicating that C1B–C2 dissociates from membranes upon sequestration of metal ions. In Pb^{2+} experiments, the intensity of the Trp peak does not fully recover upon EGTA treatment because C2 has one high-affinity Pb^{2+} site[9] that remains populated. We were surprised to find that Cd^{2+} supported the membrane association of C1B–C2 oligomers (Figure 3F), because we knew from previous work that, unlike Pb^{2+}, Cd^{2+} binding to the isolated C2 domain does not drive the membrane association (inset of Figure 3F and ref 10). The most plausible explanation for the enhancement of membrane-binding affinity of the C1B–C2 oligomers is the increase in the effective concentration of C2 membrane-binding functionalities in the oligomers. We recently observed a similar behavior for the two C2 domains of Synaptotagmin I,[21] where a high local concentration was created through protein tethering to the membranes via the N-terminal segment.

There exists experimental evidence that Ca^{2+} binding to the C2 domain can facilitate self-association of PKCα.[25,26] We previously demonstrated, using NMR relaxation techniques, that Ca^{2+}-dependent dimerization of the isolated C2 domain in solution is extremely weak, with ~2–3% population of dimeric species.[27] Similarly, our Ca^{2+}/C1B–C2 SAXS (Figure 2) and EM data (Figure S1) indicate that Ca^{2+} does not cause significant self-association of C1B–C2. The sharp contrast between Ca^{2+}- and Cd^{2+}/Pb^{2+}-dependent behaviors of C1B–C2 suggested that xenobiotic metal ions act through a mechanism that is distinct from Ca^{2+}. To gain insight into the mechanism of Cd^{2+}- and Pb^{2+}-driven self-assembly, we used 2D ^{15}N–^{1}H NMR spectroscopy.

Treatment of C1B–C2 with Cd^{2+} and Pb^{2+} resulted in (i) ^{1}H and ^{15}N chemical shift changes due to Cd^{2+} and Pb^{2+} binding to the C2 loops, consistent with our previous findings;[9,10] (ii) progressive decrease in cross-peak intensities due to self-assembly; and (iii) extreme attenuation of the backbone N–H cross-peak intensities in three protein regions (Figure 4A). The latter indicates that the affected residues participate in a chemical exchange process that

is intermediate on the NMR chemical shift time scale. We speculated that the broadened regions: loop 3 of the C2 domain, the C-terminal α-helix of the C2 domain, and the linker region connecting C1B and C2 may be directly involved in metal-ion-mediated self-assembly.

To test this, we first eliminated the ability of the C2 domain to coordinate metal ions, by mutating Asp246 of loop 3 to Asn (D246N), or mutating Asp187 and Asp193 of loop 1 to Asn (D187N/D193N) (see Figure 4B for the location of the residues). Size-exclusion chromatography (Figure S3A) revealed that the effect of these mutations on self-assembly is either modest (D246N) or nonexistent (D187N/D193N) (Figure S3B). We concluded that ionic mimicry, i.e. binding of Cd^{2+} and Pb^{2+} to the canonical Ca^{2+} binding sites, is not the major driving force behind the self-assembly of the N-term region.

The C-terminal α-helix has three glutamic acids, Glu281, Glu282, and Glu284, and a glutamine, Gln280. The linker region contains Asp154, His155, and Glu157 (Figure 4B). All of these residues can potentially coordinate divalent metal ions. We reasoned that if indeed these regions contribute to the intermolecular coordination of Cd^{2+} and Pb^{2+}, the mutation of charged residues would reduce the extent of self-assembly. Charge reversal of three acidic residues: Asp154, Glu157, and Glu281 and replacement of His155 with Gly resulted in a significant increase in monomeric C1B–C2 species (Figure S3C).

We then constructed a “Linker-Helix” (LH) C1B–C2 variant, in which we replaced the entire linker region with glycines and reversed the charge of the α-helix by replacing the three glutamic acids with lysines. The ^{15}N-filtered ^{1}H NMR spectra in the presence of Cd^{2+} (Figure 4C) and Pb^{2+} (Figure 4D) clearly show that while in the wild-type C1B–C2 the integrated intensity of amide region decreases due to self-assembly; no such decrease is observed in the LH variant. Consistent with the NMR results, the LH elutes from the size-exclusion columns as monomeric species, in contrast to the mostly oligomeric wild-type C1B–C2 (Figure 4E,F).

Replacing only the linker region with glycines was not sufficient to completely abolish the self-assembly (Figure S4). In aggregate, our data indicate that both the linker region connecting C1B and C2 and the α-helix of the C2 domain are the major drivers of the C1B–C2 self-assembly. These regions are highly conserved in all Ca^{2+}-dependent PKC isoenzymes across different species (Figure S5). The C1B domain does not appear to have a significant role in the self-assembly of the N-term region. According to our NMR data, structural integrity of C1B is not perturbed by treatment with Cd^{2+} and Pb^{2+}.

In summary, Cd^{2+}- and Pb^{2+}-driven self-assembly of the N-term regulatory region is the most unexpected and surprising finding of our study. The implication of our results is that, in addition to ionic mimicry, one of the mechanisms of Pb^{2+} and Cd^{2+} toxicity could be the clustering of proteins at the membrane surface. Using sedimentation velocity experiments, we estimated that the apparent affinity of Cd^{2+}-driven self-association is $< 7\ \mu M$ at a physiological pH of 7.4 (Figure S6). This is comparable to the 5–40 μM range reported for the peptoid ligands that were specifically designed for Cd^{2+} sequestration from biological fluids.[28] The C1B–C2 system, specifically the amino acid composition of regions mediating

self-assembly, can therefore provide a useful biological template for designing highly efficient sequestration agents that are free of limitations associated with chelation therapy. Finally, our data and recent reports[29–31] on the supra-molecular ring structures of C2 domains from Synaptotagmin 1 suggest that Ca^{2+}-dependent C2 domains in combination with xenobiotic metal ions could be useful building blocks for creating protein–metal-ion nanostructures.

Supplementary Material

Refer to Web version on PubMed Central for supplementary material.

Funding

This work was supported by the NIH grant R01GM108998 (T.I.I.). S.G.E. and K.A.M. were supported by the NSF CAREER award CHE-1151435 (T.I.I.).

REFERENCES

1. Faroon O, and Ashizawa A, et al. (2012) Toxicological Profile for Cadmium, U.S. Department of Health and Human Services, Public Health Service, Atlanta.
2. Abadin H, and Ashizawa A, et al. (2007) Toxicological Profile for Lead, U.S. Department of Health and Human Services, Public Health Service, Atlanta.
3. Hanna-Attisha M, LaChance J, et al. (2016) Elevated blood lead levels in children associated with the flint drinking water crisis: a spatial analysis of risk and public health response. Am. J. Public Health 106, 283–290. [PubMed: 26691115]
4. Lo YC, Dooyema CA, et al. (2012) Childhood lead poisoning associated with gold ore processing: a village-level investigation-Zamfara State, Nigeria, October-November 2010. Environ. Health Perspect 120, 1450–1455. [PubMed: 22766030]
5. Dalton TP, He L, et al. (2005) Identification of mouse SLC39A8 as the transporter responsible for cadmium-induced toxicity in the testis. Proc. Natl. Acad. Sci. U. S. A 102, 3401–3406. [PubMed: 15722412]
6. Chang Y-F, Teng H-C, et al. (2008) Orai1–STIM1 formed store-operated Ca2+ channels (SOCs) as the molecular components needed for Pb^{2+} entry in living cells. Toxicol. Appl. Pharmacol 227, 430–439. [PubMed: 18190941]
7. Bressler JP, Olivi L, et al. (2004) Divalent metal transporter 1 in lead and cadmium transport. Ann. N. Y. Acad. Sci 1012, 142–152. [PubMed: 15105261]
8. Markovac J, and Goldstein GW (1988) Picomolar concentrations of lead stimulate brain protein kinase C. Nature 334, 71–73. [PubMed: 3386747]
9. Morales KA, Lasagna M, et al. (2011) Pb^{2+} as Modulator of Protein-Membrane Interactions. J. Am. Chem. Soc 133, 10599–10611. [PubMed: 21615172]
10. Morales KA, Yang Y, et al. (2013) Cd^{2+} as a Ca^{2+} Surrogate in Protein-Membrane Interactions: Isostructural but Not Isofunctional. J. Am. Chem. Soc 135, 12980–12983. [PubMed: 23937054]
11. Bouton CM, Frelin LP, et al. (2001) Synaptotagmin I is a molecular target for lead. J. Neurochem 76, 1724–1735. [PubMed: 11259490]
12. Habermann E, Crowell K, et al. (1983) Lead and other metals can substitute for Ca2+ in calmodulin. Arch. Toxicol 54, 61–70. [PubMed: 6314931]
13. Kursula P, and Majava V (2007) A structural insight into lead neurotoxicity and calmodulin activation by heavy metals. Acta Crystallogr., Sect. F: Struct. Biol. Cryst. Commun 63, 653–656.
14. Simons TJ (1995) The affinity of human erythrocyte porphobilinogen synthase for Zn^{2+} and Pb^{2+}. Eur. J. Biochem 234, 178–183. [PubMed: 8529638]
15. Erskine PT, Senior N, et al. (1997) X-ray structure of 5-aminolaevulinate dehydratase, a hybrid aldolase. Nat. Struct. Biol 4, 1025–1031. [PubMed: 9406553]

16. Carpenter M, Shah AS, et al. (2016) Thermodynamics of Pb (II) and Zn (II) binding to MT-3, a neurologically important metallothionein. Metallomics 8, 605–617. [PubMed: 26757944]
17. Pinter TB, Irvine GW, et al. (2015) Domain selection in metallothionein 1a: Affinity-controlled mechanisms of zinc binding and cadmium exchange. Biochemistry 54, 5006–5016. [PubMed: 26167879]
18. Sun X, Tian X, et al. (1999) Analysis of differential effects of Pb^{2+} on protein kinase C isozymes. Toxicol. Appl. Pharmacol 156, 40–45. [PubMed: 10101097]
19. Beyersmann D, Block C, Malviya AN, et al. (1994) Effects of cadmium on nuclear protein kinase C. Environ. Health Perspect 102 (Suppl 3), 177–180.
20. Long GJ (1997) The effect of cadmium on cytosolic free calcium, protein kinase C, and collagen synthesis in rat osteosarcoma (ROS 17/2.8) cells. Toxicol. Appl. Pharmacol 143, 189–195. [PubMed: 9073607]
21. Katti S, Nyenhuis SB, et al. (2017) Non-Native Metal Ion Reveals the Role of Electrostatics in Synaptotagmin 1-Membrane Interactions. Biochemistry 56, 3283–3295. [PubMed: 28574251]
22. Katti S, Her B, et al. (2018) High affinity interactions of Pb^{2+} with synaptotagmin I. Metallomics 10, 1211–1222. [PubMed: 30063057]
23. Cole TR, and Igumenova TI (2015) Expression and purification of the N-terminal regulatory domain of Protein Kinase C for biophysical studies. Protein Expression Purif. 110, 14–21.
24. Durand D, Vives C, et al. (2010) NADPH oxidase activator p67(phox) behaves in solution as a multidomain protein with semi-flexible linkers. J. Struct. Biol 169, 45–53. [PubMed: 19723583]
25. Swanson CJ, Sommese RF, et al. (2016) Calcium Stimulates Self-Assembly of Protein Kinase C alpha In Vitro. PLoS One 11, No. e0162331. [PubMed: 27706148]
26. Bonny M, Hui X, et al. (2016) C2-domain mediated nano-cluster formation increases calcium signaling efficiency. Sci. Rep 6, 36028. [PubMed: 27808106]
27. Morales KA, Yang Y, et al. (2016) Dynamic Response of the C2 Domain of Protein Kinase $C\alpha$ to Ca^{2+} Binding. Biophys. J 111, 1655–1667. [PubMed: 27760353]
28. Knight AS, Zhou EY, et al. (2015) Development of peptoid-based ligands for the removal of cadmium from biological media. Chemical science 6, 4042–4048.
29. Wang J, Bello O, et al. (2014) Calcium sensitive ring-like oligomers formed by synaptotagmin. Proc. Natl. Acad. Sci. U. S. A 111, 13966–13971. [PubMed: 25201968]
30. Wang J, Li F, et al. (2017) Circular oligomerization is an intrinsic property of synaptotagmin. eLife 6, No. e27441. [PubMed: 28850328]
31. Zanetti MN, Bello OD, et al. (2016) Ring-like oligomers of Synaptotagmins and related C2 domain proteins. eLife 5, No. e17262. [PubMed: 27434670]

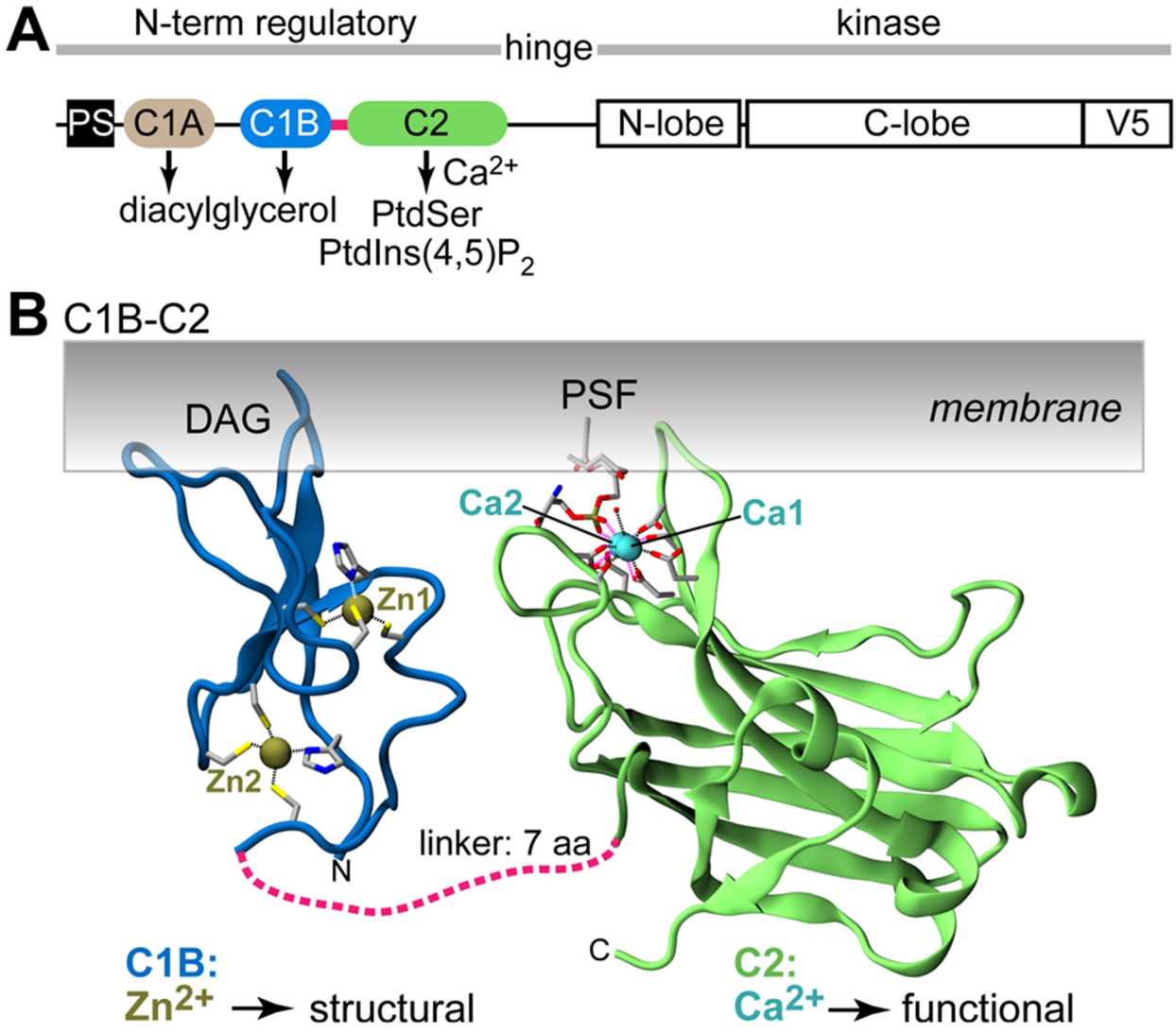

Figure 1.

Modular structure (A) and peripheral domains of conventional PKC isoenzymes (B). Shown is the ribbon representation of C1B (NMR structure, 2ELI) with highlighted structural Zn^{2+} sites, and C2 (crystal structure, 1DSY) in complex with Ca^{2+} and phosphatidylserine analogue, PSF. DAG stands for diacylglycerol.

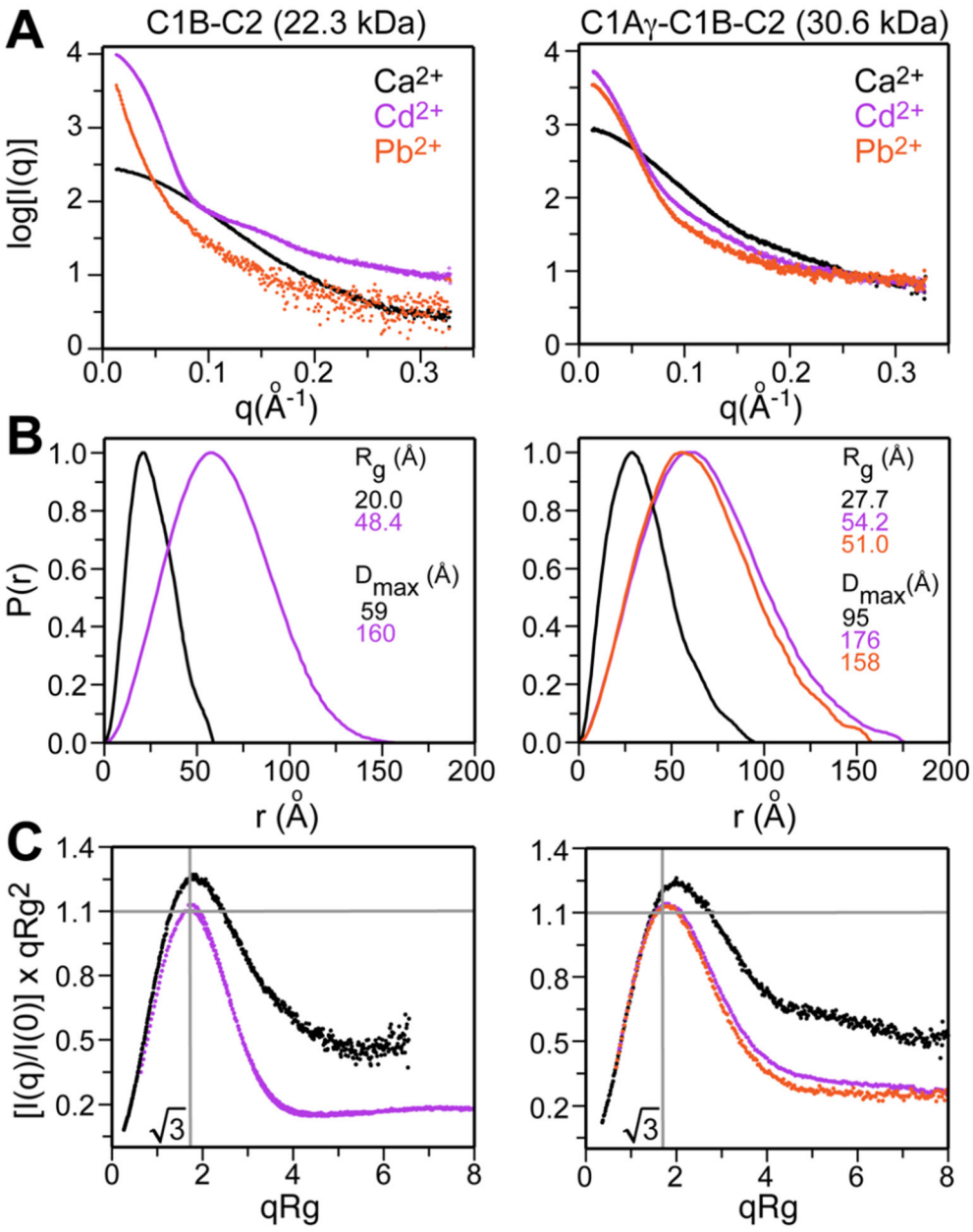

Figure 2.

Cd^{2+}- and Pb^{2+}-induced C1B–C2 self-association results in loss of conformational flexibility and formation of globular species.(A) SAXS scattering curves of the 2- and 3-domain regulatory regions showing the differences between Ca^{2+}- and Cd^{2+}/Pb^{2+}-bound proteins. Changes in size and flexibility/shape caused by Cd^{2+} and Pb^{2+} are evident from the comparison of pair-distance distribution functions $P(r)$ (B) and dimensionless Kratky plots (C), respectively.

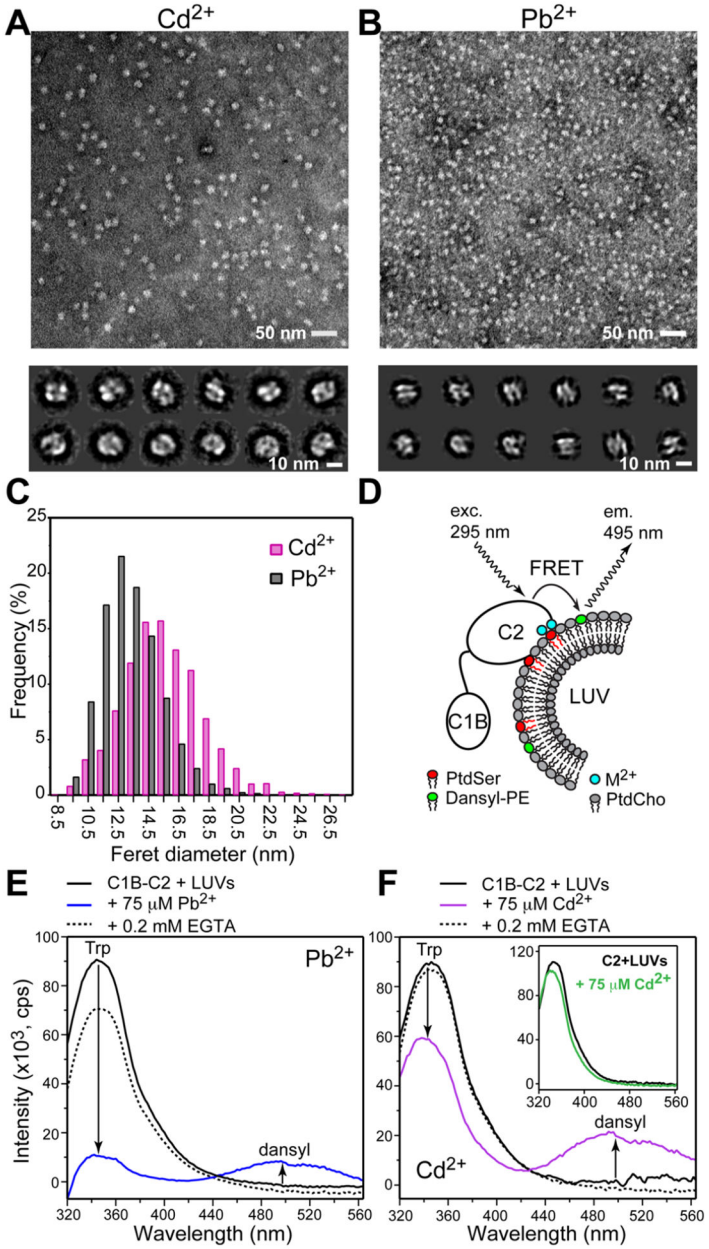

Figure 3.

Electron micrographs and class averages of (A) Cd^{2+}- and (B) Pb^{2+}-complexed C1B–C2. (C) Distribution of Feret diameters in Cd^{2+}- and Pb^{2+}-complexed C1B–C2. (D) Schematic representation of FRET experiments. C2 tryptophan residues and the dansyl-labeled lipids in the LUVs serve as a donor and acceptor, respectively. (E, F) Fluorescence emission spectra of C1B–C2 in the presence of LUVs as a membrane mimic. The appearance of dansyl emission peak at 495 nm due to membrane binding is shown with an arrow. Inset in part F: spectra of the isolated C2 domain in the presence of LUVs and Cd^{2+}.

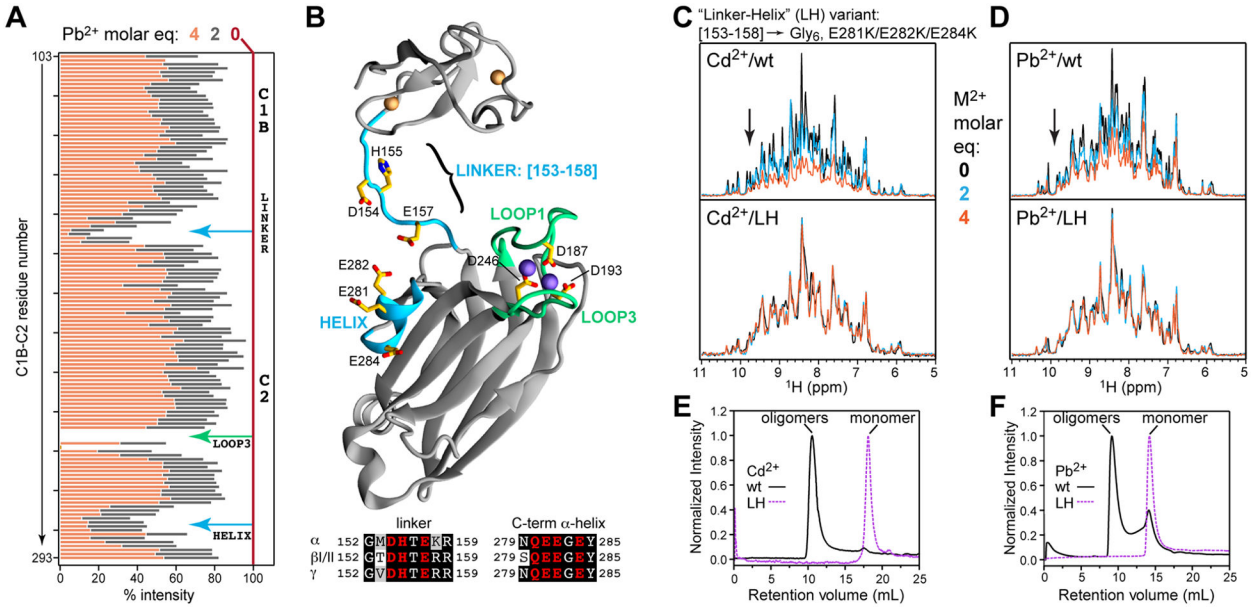

Figure 4.

Self-assembly is mediated by noncanonical metal-ion-binding motifs. (A) Normalized intensities of the N–H backbone cross-peaks in Pb^{2+}-complexed C1B–C2. Arrows indicate three regions that show extreme broadening. (B) Ribbon representation of C1B–C2 with a modeled linker region. Cd^{2+} and Zn^{2+} are depicted as purple and tan spheres, respectively. Also shown is the sequence alignment of the linker and helical regions in conventional PKCs, with putative Cd^{2+}- and Pb^{2+}-coordinating residues highlighted in red. (C, D) ^{15}N-filtered ^{1}H NMR spectra of the amide region in wild-type C1B–C2 and its LH variant. (E, F) Size-exclusion chromatography of C1B–C2 and its LH variant in the presence of Cd^{2+} (E, Superdex 200 Increase 10/300) and Pb^{2+} (F, Superdex 75 10/300 GL). The population of oligomeric species is dominant in the wild-type species, but is undetectable in the LH variant.